ISSN 1330-3651 (Print), ISSN 1848-6339 (Online)
https://doi.org/10.17559/TV-20230825000897
Original scientific paper

Study of Multilayer Welded Structure Made of AISI 316LSi Using WAAM

Katarína BÁRTOVÁ*, Jozef BÁRTA, Jana PTAČINOVÁ

Abstract: The current era makes a pressure on more ecological and economical production, therefore technological innovations are required. Current trend is to use additive manufacturing, which saves production time and reduces the amount of waste. That also contributes to better utilization of raw materials. This paper deals with the analysis of multilayer weld made of AISI 316LSi using WAAM. The aim was to evaluate the integrity of this component via structural analysis. A pipe was welded up and the cross-section of the pipe was analysed using optical microscopy and scanning electron microscopy. The microstructure of the weld metal revealed a dendritic morphology. The dendrites were formed by austenite and the interdendritic space contained δ-ferrite. The boundaries of individual weld layers were sharp and without the presence of an annealed area. SEM-EDS analysis was used in order to obtain maps of the elements distribution in examined microstructure. Globular particles were observed in the microstructure. These particles were identified as oxides rich in silicon and manganese. The mechanical properties were evaluated using microhardness measurement in vertical line and three horizontal lines of the wall. It was found that the microhardness values in the top and middle part of the wall are higher on the inside of the component due to cooling conditions.

Keywords: AISI 316LSi; EDS; microstructure; MIG; SEM; WAAM

1 INTRODUCTION

At the beginning of the new millennium, one of the main priorities of companies around the world became productivity. However, current trend is also towards more ecological production and cost-saving through material saving. One of the most important technologies of the last years is Additive Manufacturing (AM) [1-3]. AM uses a digital platform to apply material layer by layer to produce the resulting 3D component. This unique feature makes it a reliable and innovative technique that produces a component directly from CAD (computer aided design) data. Expensive tools such as casting moulds are not required anymore. It enables easy production of various complex geometries. In low-volume production, it significantly reduces costs and time [4]. AM utilizing arc welding technologies is attracting the attention of the industry for its ability to produce large metal components in a short time, at low cost and at a high material deposition rate [5].

Figure 1 Successful examples illustrating the potential of WAAM in steel construction. a) Truss structure with optimised member sizes; b) connection of spatial shells; c) the bridge in Darmstadt; d) MX3D bridge in Amsterdam [5]

AM using arc welding methods has been the subject of many studies over the past three decades. The concept of using electric arc welding methods to build components layer by layer was initiated in the 1990s in Europe. Many researches were devoted to simulation [6-9] of the process as well as to mechanical properties [9-16]. AISI 316LSi austenitic stainless steel is widely used in aerospace, marine, nuclear plant and chemical processing industries because of its excellent corrosion resistance [17-18]. By welding several components with good structural integrity and mechanical properties, the suitability of this concept for additive manufacturing of metal materials was proven. Nevertheless, compared to other AM methods of metallic materials, WAAM (Wire Arc Additive Manufacturing) has received less attention for the following reasons:

- The introduced heat associated with the electric arc can cause residual stresses and deformations, thus heat treatment may be required.
- Processing of the resulting component is often necessary (at least functional surfaces).
- Solid layers cannot be filled in such a way that they form a smooth surface, creating internal gaps and cavities.
- Automation process from the CAD model to the actual part is not elaborated enough and needs specific control to ensure wall stability.
- Lack of integrated and reliable process monitoring and control systems, which would be able to react to changes during layer deposition.
- Lower precisions compared to other WAAM technologies, e.g. laser sintering of laser metal deposition.

The mentioned shortcomings are the subject of numerous studies, thanks to which the WAAM method is constantly being improved. At the same time, the WAAM method also brings benefits compared to other AM methods, which include:

- Elimination of the need for powder recycling.
- Considerably lower price of starting material in the form of wire compared to powder.
- Lower price of equipment.
- Easy production of large-scale components and no restrictions related to size of processing chamber.

The WAAM method has seen many innovations and modifications since its inception, yet it has not been industrially commercialized worldwide [4]. The study of

the properties of components made of CrNi steels produced by the WAAM method will contribute to the further development of this promising method of additive manufacturing.

2 MATERIALS AND METHODS

The aim of the experiment is to produce and analyse the component in the shape of the pipe with the diameter of 60 mm and 50 mm length using WAAM. The material applied to the MIG welding process was OK AutrodAISI 316LSi in the form of wire with a diameter of 1.2 mm. Typical chemical composition of the AISI 316LSi filler wire is provided in Table 1.

Table 1 Typical chemical composition of OK AutorodAISI 316LSi

C	Mn	Si	Ni	Cr	Mo	Cu
0.01	1.8	0.9	12.2	18.4	2.60	0.12

Setup used for the experiment is illustrated in Figure 2. Rotational movement of the support plate was realised by rotary positioner, while welding torch movement was realised only in vertical axis. Support pipe was welded to the bottom of the plate in order to fix a plate to a chuck. Welding machined used in this experiment was Fronius TPS600i with argon (4.6) as a shielding gas.

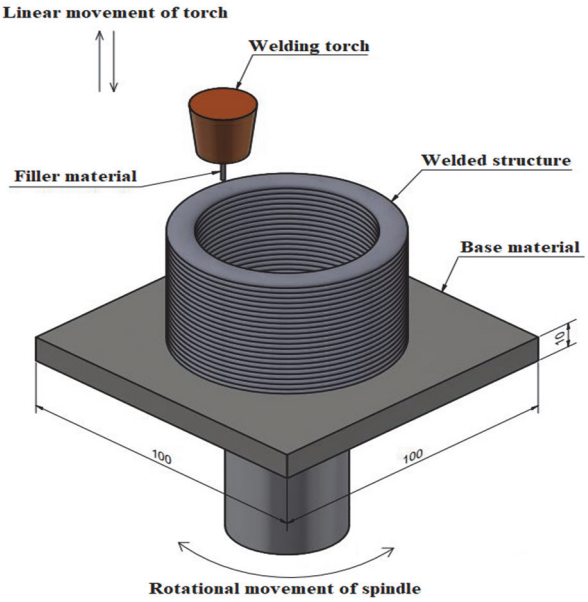

Figure 2 Experimental setup

3 RESULTS

Process parameters were set up to achieve the stable wall thickness bigger than 8 mm. Reason is to get 5 mm after machining process later on (not a part of this paper). First attempt to weld up the stable wall failed on excessive heat input. The first layer of weld was successfully connected to base material, however the 2nd pass using same parameters exhibited too high heat input since the weld pool got too big and molten pool leaked out from planned trajectory and therefore devalued the sample. Because of this, parameters were adjusted in next sample. Since original parameters exhibited a good connection to base material, same parameters were used for 1st layer of 2nd sample. All other passes had reduced parameters in order to get lower heat input and better stability of the wall. To meet these requirements, welding parameters provided in Table 2 were used.

Table 2 Welding parameters

Welding parameter	1st pass	2nd - *n* weld
Current / A	235	175
Voltage / V	24.6	21.5
Welding speed / mm/s	5	5
Feeding speed / m/min	8.0	6.0
Torch distance / mm	12	
Shielding gas (Argon) / l/min	20	

These parameters proved to be suitable to weld up a stable wall of the pipe (Figure 3). Visually, the wall did not show any abnormalities. Welding was not realised continually, since interpass temperature of 100 °C was included to avoid previous issues with high heat input. Sample was rotated for 90° after every weld pass, so it would not start all the time at the same point. This way the issues with irregularities when process starts and ends were avoided and did not stack on each other.

Figure 3 Welded up pipe

The narrowest width measured in upper part of cross-section was 8.2 mm (Figure 4). Both width and length of the pipe wall were suitable. Sample was prepared using standard metallographic procedure and electrolytical etching in 10% oxalic acid for 15 seconds.

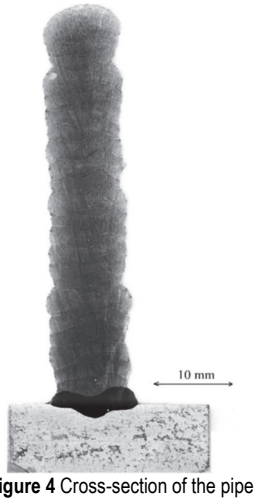

Figure 4 Cross-section of the pipe

The microstructure of wall was firstly recorded using the light microscope NEOPHOT 32. The microstructure of the weld metal in wall axis (Figure 5) showed dendritic morphology due to the absence of a phase transformation associated with a change in the crystal structure.

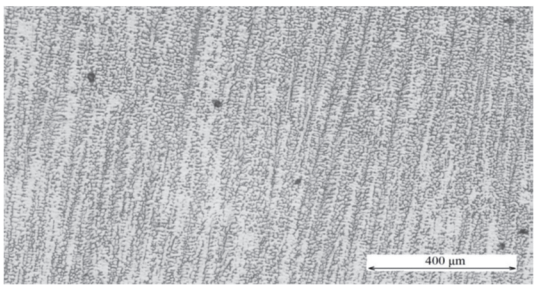

Figure 5 Microstructure of weld metal in wall axis

Dendrites were oriented vertically due to the direction of heat dissipation. The dendrites were formed by austenite and the interdendritic space was formed by δ-ferrite. The boundaries of the individual weld layers were sharp and without the presence of an annealed area. Dendrites have a coaxial vertical orientation across the interface between the layers (Figure 6).

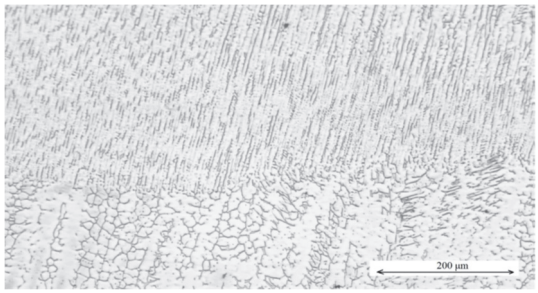

Figure 6 Transition between two weld passes

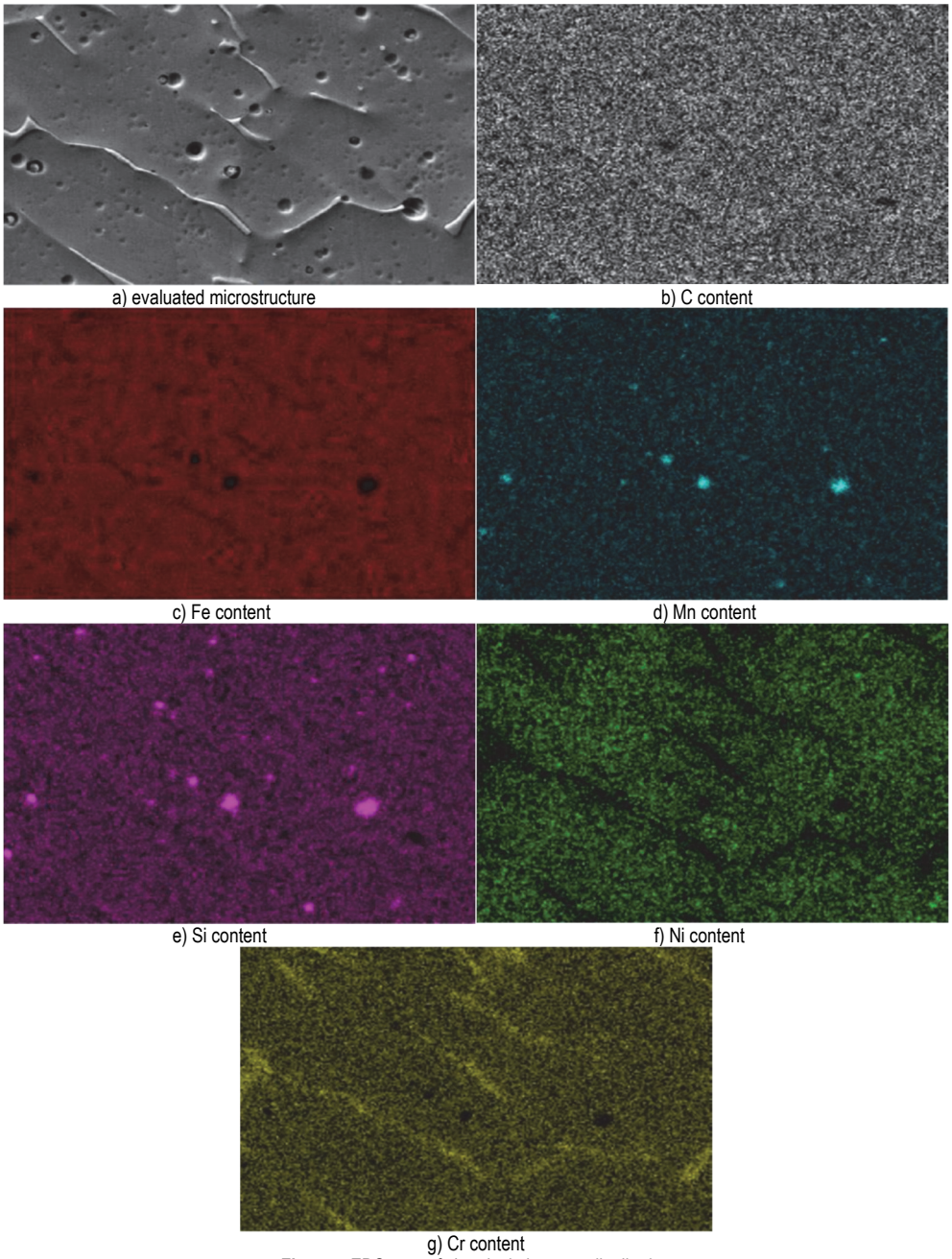

a) evaluated microstructure
b) C content
c) Fe content
d) Mn content
e) Si content
f) Ni content
g) Cr content

Figure 7 EDS map of chemical elements distribution

The orientation of the dendritic grains differed on the edge of the wall since predominant heat dissipation was towards its edge. For the scanning electron microscopy (SEM), a JEOL JSM7600F microscope equipment with Oxford Instruments EDS-detector was used, whereas the microstructure was recorded using secondary electron (SE)

detection regimes. Figure 7 documents the microstructure and map of chemical elements distribution, realised in weld metal. Globular particles rich in Mn and Si were observed. Several dark places lacking iron and carbon were observed. Due to this fact, it can be stated that those are oxides. Uniform distribution of iron and carbon was observed, which means that there were no carbides in the given microstructure. In the case of chromium, it showed greater presence in the interdendritic regions of δ-ferrite. Nickel was mostly present in austenite region. In the case of silicon and manganese, their greater presence can be observed where oxides are likely to be found in the given microstructure. Since an EDS map was not realised for oxygen, it cannot be claimed that these are oxides. Point EDS analysis was realised to confirm it (Figure 8, Table 3).

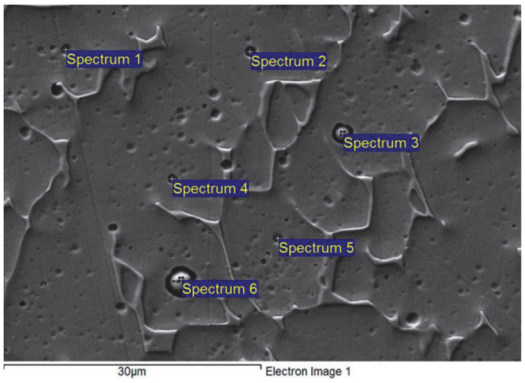

Figure 8 Microstructure for EDS point analysis

Table 3 Measured chemical composition in particular spectrums

Sp	Element / hm. %							
	C	O	Si	Cr	Mn	Fe	Ni	Mo
1	7.89	4.25	2.14	15.9	4.17	53.5	10.3	1.87
2	6.93	17.3	7.97	11.8	14.6	34.2	5.88	1.42
3	7.75	40.3	16.2	4.11	26.7	3.30	0.42	1.27
4	7.87	23.3	9.93	9.54	17.2	26.8	4.30	1.18
5	6.07	0.61	0.60	17.1	1.82	60.7	11.2	1.85
6	5.56	37.7	21.6	2.83	29.5	2.22	0.00	0.50

Spectra no. 3 and 6 in Table 3 have a significantly increased content of oxygen, silicon and manganese, thanks to which it can be concluded that these are oxides rich in silicon and manganese. At the same time, spectra no. 3 and 6 had significantly lower content of iron and chromium compared to spectra 1, 2, 4 and 5. Spectra no. 3 and 6 were realised on place where oxides were present, while spectra no. 1, 2, 4, and 5 were realised in cavities left probably by oxides that fell out during etching process of metallographic preparation.

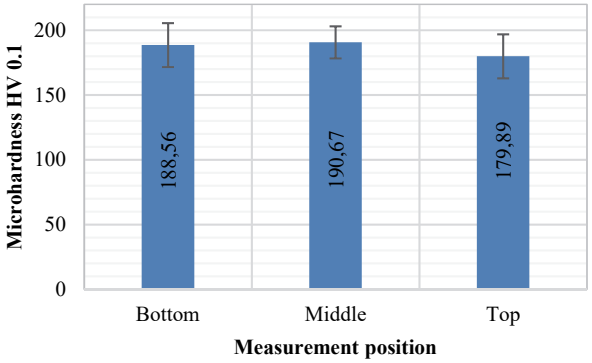

Figure 9 Microhardnes measurements in 3 horizontal lines

Microhardness of the sample was measured by Indentamet 1100 in three horizontal (top, middle and bottom) lines and one vertical in wall axis. Microhardness in horizontal lines was measured across the wall thickness. Together nine measurements were made for every line. Average values with standard deviation are provided in Figure 9. Total average value in horizontal measurements was 186.37 HV0.1.

Measurement in vertical line showed bigger differences. The differences in measurement were caused by different position of the indent (weld metal or annealed zone). Weld metal showed the average value of 176 HV0.1 based on 12 measurements, measured every 5 mm.

4 CONCLUSION

Based on the results observed during the experiment, following statements can be made:

- to avoid leak of the weld metal during welding, interpass temperature shall be used,
- welding should not start and end in same position in order to overcome problems with stacking errors at the beginning and ending of the welding process,
- following these rules, it was possible to obtain stable wall thickness bigger than 8 mm,
- structure of the weld metal is dendritic, having austenite dendrites and δ-ferrite in interdendritic space,
- presence of oxides rich in silicon and manganese were confirmed by EDS analysis,
- microhardness measurement, measured in top, middle and bottom section did not show any abnormalities,
- average microhardness of horizontal measurements was 186.37 HV0.1, whereas only 176 HV0.1 microhardness was measured in vertical line.

Despite the fact that chromium content showed in Fig. 7g showed relatively uniform distribution, slightly higher content was observed in interdendritic space. Therefore, further experiments will be focused on corrosion resistance.

Acknowledgement

This work was supported by Operational Programme Integrated Infrastructure, funded by the European Regional Development Fund. "Development of new progressive cutting tools for machining parts produced by WAAM additive manufacturing technology to reduce the number of cutting tools when machining parts from different types of materials" (ITMS2014+: 313011BWQ8)

5 REFERENCES

[1] Senthil, T. S., Babu, S. R., Puviyarasan, M., & Balachandar, V. S. (2023). Experimental investigations on the multi-layered SS316L wall fabricated by CMT-based WAAM: Mechanical and microstructural studies. *Journal of alloys and metallurgical systems*, *2*, 100013. https://doi.org/10.1016/j.jalmes.2023.100013

[2] Tankova, T., Andrade, D., Branco, R., Zhu, C., Rodrigues, D., & Simões da Silva, L. (2022). Characterization of robotized CMT-WAAM carbon steel. *Journal of constructional steel research*, *199*, 107624. https://doi.org/10.1016/j.jcsr.2022.107624

[3] Koli, Y., Aravindan, S., & Rao, P. V. (2022). Influence of heat input on the evolution of δ-ferrite grain morphology of SS308L fabricated using WAAM-CMT. *Mater charact*, *194*, 112363. https://doi.org/10.1016/j.matchar.2022.112363

[4] Tomar, B., Shiva, S., & Nath, T. (2022). A review on wire arc additive manufacturing: Processing parameters, defects, quality improvement and recent advances. *Mater today commun*, *31*, 103739. https://doi.org/10.1016/j.mtcomm.2022.103739

[5] Evans, S. I., Wang, J., Qin, J., He, Y., Shepherd, P., & Ding, J. (2022). A review of WAAM for steel construction-Manufacturing, material and geometric properties, design, and future directions. *Structures*, *44*, 1506-1522. https://doi.org/10.1016/j.istruc.2022.08.084

[6] Zhao, W., Tashiro, S., Murphy, A. B., Tanaka, M., Liu, X., & Wei, Y. (2023). Deepening the understanding of arc characteristics and metal properties in GMAW-based WAAM with wire retraction via a multi-physics model. *J. manuf. process*, *97*, 260-274. https://doi.org/10.1016/j.jmapro.2023.05.008

[7] Zhao, W., Wei, Y., Tashiro, S., Tanaka, M., & Murphy, A. B. (2023). Numerical investigations of arc plasma characteristic parameters evolution and metal properties in GMAW-based WAAM of Al alloy with an integrated model. *J. manuf. process*, *99*, 321-337. https://doi.org/10.1016/j.jmapro.2023.05.047

[8] Ling, Y., Ni, J., Antonissen, J., Hamouda, H. B., Voorde, J. V., & Wahab, M. A. (2023). Numerical prediction of microstructure and hardness for low carbon steel wire Arc additive manufacturing components. *Simul. model practtheory*, *122*, 102664. https://doi.org/10.1016/j.simpat.2022.102664

[9] Krishnaveni, S., Kunchala, B. R., Gamini, S., & Ch Anilkumar, T. (2023). Machine learning-based bead modeling of wire arc additive manufacturing (WAAM) using an industrial robot. *Mater. today proc.* https://doi.org/10.1016/j.matpr.2023.04.534

[10] Wang, J., Zhu, K., Zhang, W., Zhu, X., & Lu, X. (2023). Microstructural and defect evolution during WAAM resulting in mechanical property differences for AA5356 component. *Journal of materials research and technology*, *22*, 982-996. https://doi.org/10.1016/j.jmrt.2022.11.116

[11] Vora, J., Parmar, H., Chaudhari, R., Khanna, S., Doshi, M., & Patel, V. (2022). Experimental investigations on mechanical properties of multi-layered structure fabricated by GMAW-based WAAM of SS316L. *Journal of materials research and technology*, *20*, 2748-2757. https://doi.org/10.1016/j.jmrt.2022.08.074

[12] Zhan, X., Wang, Q., Wang, L., Gao, Z., & Yang, X. (2022). Regionalization of microstructure and mechanical properties of Ti6Al4V transition area fabricated by WAAM-LMD hybrid additive manufacturing. *J .alloys compd*., *929*, 167345. https://doi.org/10.1016/j.jallcom.2022.167345

[13] Chen, Z. & Soh, G. S. (2022). Microstructure and mechanical properties of Wire Arc Additive Manufactured (WAAM) Inconel 718 parts via post heat treatments. *Mater today proc*, *70*, 567-573. https://doi.org/10.1016/j.matpr.2022.09.592

[14] Huang, Y., Yang, L., & Xin, Q. (2023). Novel geometrical model and design mechanical parameters for CMT-WAAM stainless steel. *J.constr.steel res*., *210*, 108071. https://doi.org/10.1016/j.jcsr.2023.108071

[15] Wang, C., Zhu, P., Wang, F., Lu, Y. H., & Shoji, T. (2022). Anisotropy of microstructure and corrosion resistance of 316L stainless steel fabricated by wire and arc additive manufacturing. *Corros. sci.*, *206*, 110549. https://doi.org/10.1016/j.corsci.2022.110549

[16] Xu, X., Ganguly, S., Ding, J., Guo, S., Williams, S., & Martina, F. (2018). Microstructural evolution and mechanical properties of maraging steel produced by wire + arc additive manufacture process. *Mater. charact.*, *143*, 152-162. https://doi.org/10.1016/j.matchar.2017.12.002

[17] Maric, D., Cumin, J., Solic, T., & Samardzic, I. (2022). Quality Analysis of AISI 321 Welds of Bellow Compensators Used in Shipbuilding. *Mar. sci. eng.*, *10*, 452. https://doi.org/10.3390/jmse10040452

[18] Kojundžić, D., Krnić, N., Samardžić, I., & Konjatić, P. (2022). Influence of Purging Gas on 316L Stainless Steel Fusion Zone in Autogenous Stationary TIG Welding. *Technical gazette*, *29*(4), 1080-1088. https://doi.org/10.17559/TV-20220407215830

Contact information:

Katarína BÁRTOVÁ, Ing., PhD
(Corresponding author)
Slovak University of Technology in Bratislava,
Faculty of Materials Science and Technology in Trnava,
Jána Bottu 25, 917 24 Trnava, Slovakia
E-mail: katarina.bartova@stuba.sk

Jozef BÁRTA, Assoc. Prof., Ing., PhD, IWE
Slovak University of Technology in Bratislava,
Faculty of Materials Science and Technology in Trnava,
Jána Bottu 25, 917 24 Trnava, Slovakia
E-mail: jozef.barta@stuba.sk

Jana PTAČINOVÁ, Ing., PhD.
Slovak University of Technology in Bratislava,
Faculty of Materials Science and Technology in Trnava,
Jána Bottu 25, 917 24 Trnava, Slovakia
E-mail: jana.ptacinova@stuba.sk